Rangeland Ecology & Management 69 (2016) 481–490

Contents lists available at ScienceDirect

Rangeland Ecology & Management

journal homepage: http://www.elsevier.com/locate/rama

Ecological Site-Scale Hydrologic Response in a Semiarid Rangeland Watershed☆

Austin M. Carey [a,*], Ginger B. Paige [b]

[a] Graduate Research Assistant, Wyoming Center for Environmental Hydrology and Geophysics, University of Wyoming, Laramie, WY 82071, USA
[b] Associate Professor, Department of Ecosystem Science and Management, University of Wyoming, Laramie, WY 82071, USA

ARTICLE INFO

Article history:
Received 29 March 2016
Received in revised form 6 June 2016
Accepted 23 June 2016

Key Words:
ecological sites
infiltration
rainfall simulation
runoff

ABSTRACT

Rangelands, due to their large expanse, are responsible for processing a significant portion of freshwater in the western United States. Rangeland managers are in need of methods to quantify hydrologic processes and scientifically based decision tools to effectively manage water resources under growing populations and a changing climate. The ecological site (ES) concept provides a useful framework to study complex rangeland hydrological processes in order to parameterize these tools. Traditionally, rangeland hydrology has been studied at the plot and watershed scale. ESs are intermediate-scale land units considered to have homogeneous site characteristics, which allow for mapping the spatial variability of hydrologic processes at a higher resolution compared with a lumped watershed approach. We conducted 20 variable-intensity rainfall simulation experimental runs using the Walnut Gulch Rainfall Simulator to characterize the hydrologic response of four different ESs in the Upper Crow Creek Watershed in southeastern Wyoming. An analysis of variance test with post hoc comparisons showed that sites were significantly different in runoff-infiltration dynamics. Sites ranged from exhibiting a large runoff ratio of 0.44 to infiltrating the entire applied rainfall volume. Multiple linear regressions showed that, on average, 83% of the variability of key hydrologic variables across sites could be explained by significant relationships ($P \leq 0.05$) consisting of two or three ground cover variables. Beta weights for the regression variables indicated that percent cover of lesser spikemoss (*Selaginella densa* Rydb.) and bare soil were typically the most influential variables. Additional site-specific characteristics explain the remaining variability. The results from this study directly support the concept of using ESs to assess hydrologic response of rangelands. Incorporating quantitative hydrologic datasets into ecological site descriptions and decision tools should increase their utility for the management of rangeland ecosystems.

© 2016 The Society for Range Management. Published by Elsevier Inc. All rights reserved.

Introduction

Rangelands are estimated to comprise roughly 364 M ha of the western United States (USDA 2013). A substantial portion of the freshwater resources that fall in the West are processed through rangeland systems. Pressure for rangeland managers to understand hydrologic processes and quantify water yield in western rangelands is increasing in the context of increased population (Havstad et al. 2009) and climate variability (Archer and Predick 2008; Polley et al. 2013). As demand for water resources exceedingly outweighs supply, managers are in need of robust models and decision support tools that quantify the relationship between the characteristics of these rangeland systems and hydrologic processes. However, hydrologic response on rangelands is highly variable in space and time due to heterogeneities in soil, vegetation, and climatic conditions, making quantifying and modeling these processes challenging (Pilgrim et al. 1988; Pierson et al. 2002; Chauvin et al. 2011).

Ecological sites (ESs) can provide an effective means to partition rangelands into land units for the purpose of evaluating health, performing vegetation inventory, and implementing management strategies. ESs represent distinct associations of physical characteristics such as soil, topography, and climate, which produce a specific type and amount of vegetation (USDA 2013). Characteristics differentiating these sites are outlined in ecological site descriptions (ESDs) that also contain conceptual state-and-transition models (STM) to help organize complex information regarding long-term site dynamics. Ecological states are considered recognizable and relatively stable vegetation complexes, while transitions are the trajectory between states commonly triggered by disturbance or different management strategies (USDA 2013). Many studies have shown that hydrologic function (e.g., infiltration capacity, runoff generation, erosion) strongly influences the resilience of a given ecological state on rangelands (Wilcox et al. 2003; Newman et al. 2006; Turnbull et al. 2008). Resilience in this context is the ability of an ES to remain in a given state through mutually reinforcing processes (e.g., infiltration capacity) that work to dampen the effects of disturbance

☆ This research was funded by NSF (EPS-1208909), the Wyoming EPSCoR Office, and the Wyoming Center for Environmental Hydrology and Geophysics.
* Correspondence: Austin Carey, Wyoming Center for Environmental Hydrology and Geophysics, Laramie, WY 82072.
E-mail address: austinmartincarey@gmail.com (A.M. Carey).

http://dx.doi.org/10.1016/j.rama.2016.06.007
1550-7424/© 2016 The Society for Range Management. Published by Elsevier Inc. All rights reserved.

(Peterson et al. 1998). ESs therefore provide a useful framework to study the hydrological processes of rangeland systems. It has been hypothesized that an ES in a given condition or state should exhibit a characteristic hydrologic response that can be measured (Stone and Paige 2003; Stone et al. 2008). While rangeland hydrology has predominately been studied at plot (Simanton et al. 1991; Pierson et al. 1994) and watershed (Osborn and Lane 1969; Loague and Gander 1990; Wilcox et al. 1990; Flerchinger and Cooley 2000) scales, ESs can be thought of as an intermediate scale that represents the smallest land unit considered to be homogeneous in terms of site characteristics. As such, ESs represent the minimum polygon for mapping the spatial variability of hydrologic processes and have the potential to improve the ability to model rangeland systems compared with traditional lumped watershed models (Sivapalan 2003; Burns et al. 2010).

Hydrologic function of an ES has generally been inferred using subjective indicators such as percent bare ground, water flow patterns, and the presence of rills and gullies (Pyke et al. 2002; Hernandez et al. 2013; Williams et al. 2016). Williams et al. (2016) recently outlined the need to incorporate quantitative hydrologic data into ESDs, to enhance their utility for the management of rangeland ecosystems. Quantitative tools such as the Rangeland Hydrology and Erosion Model (RHEM; Nearing et al. 2011) can facilitate this effort by using diverse rangeland datasets to predict ES-specific hydrologic response (Hernandez et al. 2013; Williams et al. 2016). However, additional high-quality field observations relating hydrologic function to ESs are necessary to improve our ability to discern the characteristics that distinguish hydrologic response of ESs and improve the applicability of a model such as RHEM to a variety of different rangeland systems.

The objective of this study was to quantify the hydrologic response of four ESs in a semiarid rangeland watershed in southeastern Wyoming. Simulated rainfall was used to relate infiltration-runoff processes to important characteristics of key ESs. Sites that differ in vegetation type and amount, topographic variability, and soil properties should partition rainfall into runoff in unique and quantifiable ways. These ecohydrological relationships are important for understanding the role of specific ESs in distributing water resources in rangeland watersheds. Datasets such as these can be used to parameterize rangeland models and decision support tools, to improve the management of water resources under increased stress from population growth and a changing climate.

Methods

Study Area

This study was conducted in the Upper Crow Creek Watershed (UCCW), a 94-km^2 semiarid rangeland catchment approximately 22 km southeast of Laramie, Wyoming. It is situated in the South Platte River Basin and is part of the Pole Mountain District of the Medicine Bow National Forest. UCCW drains from northwest to southeast via two main streams: the Middle Crow Creek and the South Branch of the North Crow Creek, which empty into the Upper North Crow Reservoir and the Granite Springs Reservoir, respectively (Fig. 1). Elevations range from 2200 to 2760 m, and average annual precipitation is approximately 430 mm (Skinner et al. 1984). Grasses and shrubs are the dominant form of vegetation comprising roughly 61% of the watershed. Lodgepole (*Pinus contorta* Douglas ex Loudon) and ponderosa (*Pinus ponderosa* P & C. Lawson) pine are the dominant vegetation at the upper elevations, and the riparian areas are composed of a mixture of willow, aspen, and riparian grasses (USDA Forest Service 2013; Hayes et al. 2014). Bedrock geology is predominately coarse-grained 1.43-Ga Sherman granite batholith that deeply weathers to form a thick grus (Frost et al. 1999), while small slivers of the Casper Formation, as well as metasedimentary and metavolcanic rock, occur in the very northwest region of the watershed.

The University of Wyoming installed hydrologic instrumentation, rain gauges, and stream gauging stations (pressure transducers) in July 2009 as part of a nested watershed design (see Fig. 1). A meteorological station was established (467866.9 m east, 4562880.4 m west, and 2567 m above sea level) to collect basic climatic data (i.e., temperature, relative humidity, wind velocity, etc.). Five study sites were established, each equipped with four hillslope plots distributed across the hillslope. The plots are 6.1 m in length and 2 m in width, delimited by borders inserted a few centimeters into the soil surface. The specific location of each plot was determined on the basis of two criteria: relatively uniform slope, void of any major concavities, in the soil surface between 5% and 30% and a uniform plane at least 2 m wide. Four of the five sites represent distinct ESs in the major land resource area (MLRA) 49XA and are part of a natural rainfall-runoff study conducted by Perlinski et al. (2016). The ESs represented by these four sites are coarse upland (CU), shallow loamy (SL), shallow upland (SU), and loamy upland (LU). The fifth site represents a different state of the CU STM and is termed CU-2. These sites were chosen on the basis of areal extent and their hypothesized influence on the overall hydrologic response of the watershed. NRCS soils data, vegetation inventory, and detailed soil pits were used to verify the ES (USDA 2013). On the basis of information provided in the ESDs, we expect these sites to be in the reference state relative to their STMs (with the exception of CU-2). It must be noted, however, that ESDs are in early development for much of southeast Wyoming and this has not been directly verified.

Detailed characteristics of the ESs are presented in Table 1. The CU site is located on an alluvial fan overlaying granitic bedrock. A well-developed sandy clay loam profile with an average of 34% coarse fragments (>2 mm in diameter) typically extends to a depth of 0.6 m, at which point a

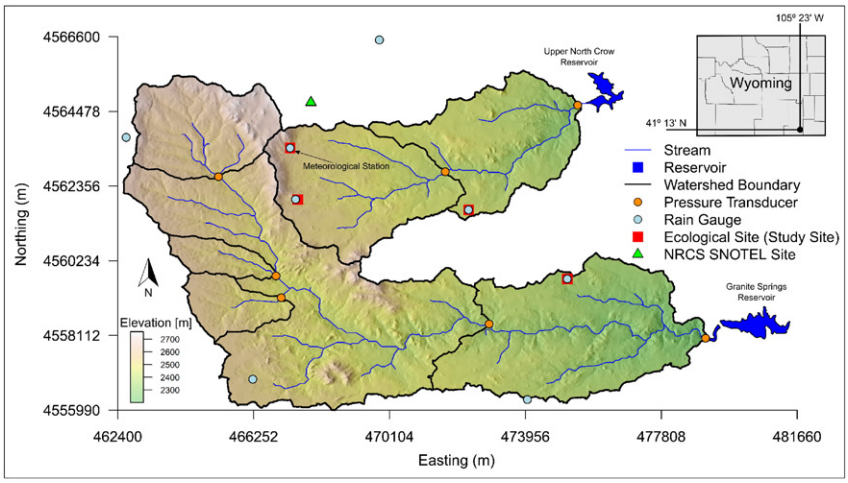

Figure 1. Map of the Upper Crow Creek Watershed (UCCW) in southeastern Wyoming. The five study sites are indicated by red squares. Hydrologic instrumentation was installed in a nested watershed design in July 2009.

Table 1
Site descriptions for the five sites.

Site characteristic	Coarse upland (CU)	Shallow loamy (SL)	Shallow upland (SU)	Loamy upland (LU)	Coarse upland 2 (CU-2)
Year Established	2009	2009	2009	2009	2015[5]
Ecological Site ID[1]	049XA108WY	049XA162WY	049XA160WY	049XA122WY	049XA108WY
Average Elevation (m)	2547	2368	2433	2567	2470
Average Slope (%)	11.5	9.6	10.7	18.6	11.9
Aspect of Hillslope Plots	South	Northwest	West	Southeast	North
Parent Material Kind[1]	Glacial Till, Alluvium	Residuum, Alluvium	Residuum, Colluvium	Residuum, Alluvium	Glacial Till, Alluvium
Parent Material Origin[1]	Granite	Granite	Granite	Sandstone	Granite
Plant Community	Wheatgrass, Bluegrass, Subshrub	Fescue, Gramma, Subshrub	Fescue, Bunch Grass, Subshrub	Dense Sagebrush, Bluegrass and Brome Understory	Wheatgrass, Fescue, Subshrub
Depth to Fractured Bedrock (m)[2]	4.0	5.8	3.7	6.1	9.6
Depth to Fresh Bedrock (m)[2]	20+	14.7	11.0	14.5	20+
Soil Map Unit[3]	Hapjack-Rogert-Amesmont complex	Boyle-Rock outcrop complex	Hapjack-Rogert-Amesmont complex	Rogert-Rock outcrop-Amesmont complex	Rogert-Rock outcrop-Amesmont complex
Surface Soil Type	Sandy Clay	Clay Loam	Sandy Clay	Loamy Sand	Sandy Clay
Profile Soil Type[4]	Sandy Clay Loam	Sandy Clay Loam	Sandy Loam	Sandy Loam	Sandy Loam
Sand, Silt, Clay (%)[4]	50, 26, 24	60, 18, 22	53, 29, 18	62, 22, 16	49, 46, 5
Coarse (>2 mm) Fragments (%)[4]	33.9	40.5	40.5	23.2	40.9
Bulk Density (g cm^{-3})[4]	1.58	1.56	1.47	1.37	1.58
Porosity (%)[4]	40.3	41.2	44.7	48.4	40.3

[1] Natural Resource Conservation Service (NRCS)—Ecological Site Description (ESD).
[2] Estimated from seismic refraction surveys.
[3] NRCS 2013.
[4] Values are for shallow soil profile.

saprolitic layer of increased coarse fragments is reached. Seismic refraction surveys indicate that fractured bedrock is about 4 m deep and fresh bedrock is > 20 m deep. Grass makes up approximately two-thirds of the vegetation with the dominant species being sandberg bluegrass (*Poa secunda* J. Presl) and bluebunch wheatgrass (*Pseudoroegneria spicata* [Pursh] Á. Löve). The remaining one-third of the vegetation is composed of subshrubs primarily threetip sagebrush (*Artemisia tripartita* Rydb.) and fringed sagewort (*Artemisia frigida* Willd.). Lesser spikemoss (*Selaginella densa* Rydb.) makes up a large portion of the ground cover at this site (32%).

The SL ecological site has a similar subsurface structure as CU with a slightly deeper saprolite layer. Fresh bedrock is typically reached at about 14.7 m. Exposed granitic boulders are common upslope of this site. There is approximately 73% canopy cover dominated by blue grama (*Bouteloua gracilis* [Willd. ex Kunth] Lag. ex Griffiths), Idaho fescue (*Festuca idahoensis* Elmer), and fringed sagewort. More than 40% of the ground cover is litter and Dalmatian toadflax (*Linaria dalmatica* [L.] Mill.) has invaded the site (<5% of the total cover).

A shallow sandy loam soil profile with more than 40% coarse fragments overlays saprolite at the SU site with many large granite boulders exposed at the soil surface. Geophysical measurements show large rotting corestones at the very near surface and the average depth to bedrock is the shallowest of all the ESs (~11 m). The plant community is dominated by bunch grasses and Idaho fescue intermixed with fringed sagewort and threetip sagebrush. More than 30% of the site is covered by a mat of lesser spikemoss, resulting in very low bare ground (~14%).

The LU ecological site is characterized by deep, highly organic loamy soils. Average depth of the soil profile at this site is typically around 0.7 − 0.8 m, but it can be as deep as 1.3 m at localized hillslope depressions. The plant community is quite dense, resulting in > 90% canopy cover. Big sagebrush (*Artemisia tridentata* Nutt.) overwhelmingly dominates the vegetation cover while robust shrubs like antelope bitterbrush (*Purshia tridentata* Pursh) and western snowberry (*Symphoricarpos occidentalis* Hook.) are also prominent. This site is also experiencing conifer encroachment, which may alter the site function.

Rainfall Simulator Experimental Runs

Infiltration and runoff processes were measured using variable-intensity rainfall simulation. The main advantage of rainfall simulators is the ability to generate a known rainfall pulse of specific magnitude and duration, for a controlled comparison of plots with different soil and vegetation parameters. In arid and semiarid environments where rainfall is infrequent and spatially variable, simulators can effectively be used to study a variety of hydrologic processes (Simanton et al. 1984; Seyfried 1991; Pierson et al. 1994; Paige and Stone 1996; Taucer et al. 2008; Stone et al. 2008).

A total of 20 rainfall simulator experimental runs were conducted (four runs at each of the five sites) during the summers of 2014 and 2015 using the Walnut Gulch Rainfall Simulator (WGRS; Paige et al. 2003). The WGRS is a portable, variable-intensity rainfall simulator developed by the USDA-ARS-Southwest Watershed Research Center to study the spatial variability of infiltration-runoff processes on rangelands at the hillslope scale (Paige et al. 2003; Stone et al. 2008). It is equipped with four VeeJet 80100 nozzles mounted to a 6-m central oscillating boom that is driven by a computer-controlled stepper motor. Water is delivered to the boom via a WT20 Honda trash pump from a nearby 1650 gal tank. An in-line pressure regulator allows for a constant outflow pressure to be set and maintained. The WGRS uses variable delay times between boom oscillations and different oscillation angles to achieve a large range (27–311 mm hr^{-1}) of applied rainfall intensities. Screens on three sides of the simulator minimize the effects of wind on rainfall distribution. Each year the simulator was calibrated before deployment in the field to verify the applied rainfall intensities and distribution across the plot.

Field runs consisted of performing two simulator runs on each plot, a dry and a wet run. All plots were equipped with instrumentation specifically designed for simulation experiments. The WGRS was positioned directly over the plots with nozzles approximately 2.4 m above the soil surface, and a constant nozzle outflow pressure of 55 kPa was maintained using a regulator to control drop size distribution and rainfall intensity. These target values for nozzle height and outflow pressure were determined to achieve the desired rainfall distributions and a rain-drop kinetic energy similar to that of natural rainfall (Paige et al. 2003). The dry runs were performed under antecedent soil moisture conditions. For all sites excluding LU, soil volumetric moisture before simulation averaged 15% (SE = 1.5%). Antecedent soil moisture for the LU site was slightly higher at 23% (SE = 5%). For the dry runs, rainfall was applied to the plots at the lowest intensity (49 mm hr^{-1} for 2014 and 53 mm

hr^{-1} for 2015) for approximately 45 minutes. This was done to establish a uniform moisture condition. After allowing time for moisture redistribution (hiatus period with no rainfall typically lasting 45 min to 1 hr), a wet run was conducted by incrementally increasing the applied rainfall using five calibrated intensities (49, 77, 112, 157, and 180 mm hr^{-1} for 2014 runs and 53, 81, 115, 153, and 181 mm hr^{-1} for 2015 runs). Surface runoff rates were continuously measured throughout both runs by routing flow from the plots through a precalibrated flume. A given rainfall intensity was applied until steady state runoff was reach for a minimum of 5 minutes, at which point the intensity was increased. A series of eight CWS655, 900-MHz, wireless reflectometer probes (Campbell Scientific, Inc., 2011, Logan, UT) were evenly distributed across the plot to monitor near surface soil moisture dynamics. Simulations for the CU and LU sites were conducted in 2014 (eight plots total), while simulations for SL, SU, and CU-2 were conducted in 2015 (twelve plots total). It typically took about a week to complete all four plot simulations for a given site.

A series of hydrologic variables were computed for all wet runs. Steady state infiltration rates (SS) for each of the five applied intensities (SS1-SS5) were calculated by subtracting the measured steady state runoff rate from the applied rainfall intensity. This represents an integrated plot-scale infiltration rate under a particular rainfall condition. Runoff coefficients (C), a unitless value defined as the fraction of rainfall that results in surface runoff, were computed by dividing the total depth of runoff by the total applied rainfall over the course of the wet run. The peak runoff rate (Q_{peak}) for the entire wet run was also noted.

Site Characteristics

Ground and vegetative canopy cover were measured for each plot post rainfall simulation using a point-intercept method (Herrick et al. 2005). Characteristics were recorded at 380 points within each plot (30-cm spacing down the length and 10-cm spacing across the plot). Canopy cover was characterized on the basis of life form, as well as species, and ground cover was classified as bare soil, rock, litter, moss, plant base, or exposed rock. To compute percent canopy cover, the first hit of the vertically descending rod was used as the frequency measurement, though multiple hits may be recorded. Bulk density and porosity were determined for each site using undisturbed soil cores (Gee and Or 2002).

Steady state infiltration rates were analyzed using a procedure presented by Hawkins (1982) and revisited by Stone et al. (2008). Assuming an exponential distribution of infiltration capacity across a given area, Hawkins derived the following equation that relates the steady-state infiltration rate to the applied rainfall rate:

$$fs(i) = \mu_f \left(1 - e^{-\frac{i}{\mu_f}}\right) \quad (1)$$

where $fs(i)$ is the steady-state infiltration rate ($L\,T^{-1}$), i is the applied rainfall rate ($L\,T^{-1}$) and μ_f is the average areal infiltration rate when the entire area under consideration is contributing to runoff ($L\,T^{-1}$). The μ_f parameter can also be thought of as the maximum spatially averaged infiltration rate for a given area. Eq. (1) suggests that steady-state infiltration increases with increasing application rate until the maximum infiltration rate (μ_f) is asymptotically reached. The spatial distribution of infiltration capacity across a given area will determine the shape of the response curve. As the applied rainfall rate increases, areas with higher infiltration capacity begin to contribute to runoff, resulting in an increase in the steady-state infiltration rate. Eq. (1) has been effectively tested using rainfall simulation data (Stone et al. 2008), as well as natural rainfall-runoff data (Yu et al. 1997). For our analysis the μ_f parameter was calculated by fitting a line through the five (i, f_S) points collected during the wet simulator run, by minimizing the root mean squared error. Using the exponential distribution of infiltration capacity, a cumulative density function can be used to compute the fraction of an area that is contributing to runoff:

$$A_C(i) = 1 - e^{-\frac{i}{\mu_f}} \quad (2)$$

where $A_C(i)$ is the fraction of the total area for a given rainfall intensity.

Statistical Analysis

Hydrologic variables of interest (i.e., SS1-SS5, C, and Q_{peak}) were compared among all five sites using a one-way analysis of variance (ANOVA) test set in a completely randomized design. Post hoc average separations were conducted using Tukey's HSD (Tukey 1953) if the F-tests indicated significant differences among sites. All data used in the ANOVA were tested for normality. The assumption of equal variances was tested using Hartley's ratio (Hartley 1950). If the variances were unequal, a weighted analysis was conducted using the inverse of the square root of the variances as weight. All ANOVA computations were performed using the GLM procedure of the Statistical Analysis System (SAS) version 9.4 (SAS Institute 2013).

Multiple linear regression was used to identify site cover characteristics that may be important in predicting the hydrologic response. Percent slope was also used in this analysis as an explanatory variable. All regressions were performed using R Statistical Software version 3.1.1 (R Development Core Team 2014). A forward selection procedure was chosen in which Pearson correlation coefficients were used to identify the starting variable for the model and subsequent variables were added to the model on the basis of partial F-tests (Kleinbaum et al. 1988). Backward procedures were also tested, in general resulting in more complex models not significantly different than forward results with poor variable inflation factors. Therefore, only the results from the forward procedure are presented. Before analysis, all data used in the regressions were tested for normality and equal variance. Model selection was performed by minimizing both the Akaike information criterion and the predictive residual sum of squares. All models discussed are significant at the $P \le 0.05$ level.

Results

Hydrographs for the wet runs from the 20 plots illustrate differences in the hydrologic response of the five ESs (Fig. 2). The SU site had the largest runoff response, indicated by the site average Q_{peak} and C values (Table 2). For all four plots runoff was generated at the lowest applied rainfall intensity (53 mm hr^{-1}). Steady-state runoff was achieved during the dry run for plots 1 and 4, indicating that these plots have an especially low infiltration capacity. Moreover, SU exhibited the lowest amount of within-site variability in runoff among all ESs. This is indicated by the similar plot hydrographs and the low standard error (SE) and coefficient of variation (CV) values for Q_{peak} and C. On average, the CU site had the second highest runoff response. Plot values for Q_{peak} and C were similar for plots 3 and 4, while slightly higher for plot 1. Substantially lower values for plot 2 led to a high degree of variability in hydrologic response across this site compared with SU. For the SL site, significant runoff did not begin until later in the experiment when soil moisture was higher and higher rainfall intensities were applied. This site exhibits a higher infiltration capacity than the SU and CU sites. While the other three sites exhibited a similar CV for Q_{peak} and C, the SL site had a significantly higher CV for C compared with Q_{peak}. This is due to plots 3 and 4, where runoff rates only began to increase toward the end of the simulation experiment. The site that exhibited the highest degree of variability in runoff generation across the hillslope was the CU-2 site. For a similar pattern in rainfall application, it can be seen that plot 1 had a Q_{peak} over 12 times greater than plot 3 and a C nearly 36 times larger. Plots 1 and 2 produce small amounts of runoff at the lowest rainfall intensity, while runoff did not begin until an intensity of 115 mm hr^{-1} for plot 3. Of all the ESs, LU overwhelmingly has the

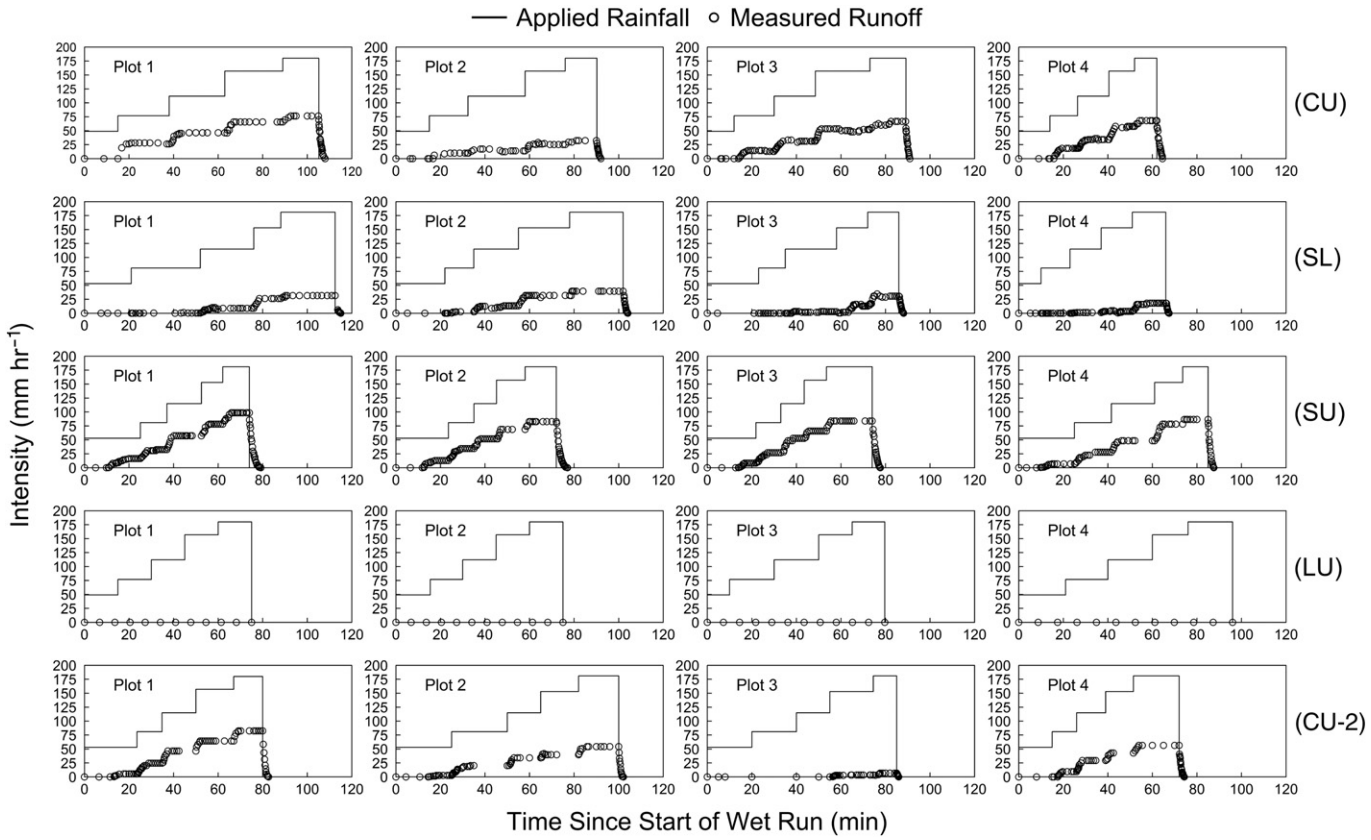

Figure 2. Hydrographs from the wet simulator runs for the five sites. Applied rainfall rate is indicated by the solid line, and measured surface runoff is shown as black circles.

largest potential to infiltrate water. This is shown by the absence of runoff during all four simulation runs. The site effectively acted as a sponge, infiltrating all rainfall that was applied.

Differences in the infiltration capacity across these sites can be seen in the areal average infiltration curves from Eqs. (1) and (2) (Fig. 3A). Variability in infiltration capacity within a given site, indicated by error bars representing the SE, follows the same trend outlined by the individual plot hydrographs. The thin, straight line in Figure 3A representing the LU site also serves as the 1:1 line in which the rainfall intensity is equally matched by the site's ability to infiltrate water. From these curves, μ_f values were calculated for each plot (Table 3). A normal site average μ_f value was calculated using all four plots, and an adjusted average was calculated excluding anomalous plots. For the CU, SL, and CU-2 sites, variability in the values of the normal averages are influenced strongly by a single anomalous plot. For example, plot 3 of the CU-2 site has a μ_f value approximately 21 times larger than the average of the remaining three plots. With these plots removed, variability in response is reduced and the adjusted averages follow the previously mentioned trend in infiltration capacity. Adjusted values were not calculated for the SU and the LU sites due to low (and in the case of LU, zero) variability in the normal μ_f averages. It is important to note that no plot during the wet simulator run ever reached its μ_f value in which 100% of the area was contributing to runoff (Fig. 3B). The SU plots were the closest to approaching this condition, with an average of 83% of the plot area

Table 2
Peak runoff rates (Q_{peak}) and runoff ratios (C) for 16 of 20 wet simulator runs. The Loamy Upland (LU) site is not shown because there was no runoff for any simulation experiment at this site. Averages, standard errors (SE), and coefficient of variations (CV) are computed for each site.

				Q_{peak}		C	
Ecological site	Plot	Q_{peak} (mm hr^{-1})	C	Average (SE)	CV (%)	Average (SE)	CV (%)
CU	1	76.4	0.38	60.9 (9.8)	32.0	0.27 (0.05)	36.3
	2	32.4	0.14				
	3	66.8	0.29				
	4	68.2	0.30				
SL	1	31.5	0.10	29.9 (4.4)	29.5	0.09 (0.03)	56.9
	2	39.5	0.15				
	3	30.6	0.06				
	4	18.1	0.04				
SU	1	98.5	0.44	87.9 (3.6)	8.3	0.40 (0.01)	6.7
	2	82.7	0.39				
	3	83.8	0.38				
	4	86.5	0.38				
CU-2	1	82.5	0.36	50.0 (15.8)	63.2	0.21 (0.07)	67.7
	2	54.3	0.24				
	3	6.7	0.01				
	4	56.4	0.24				

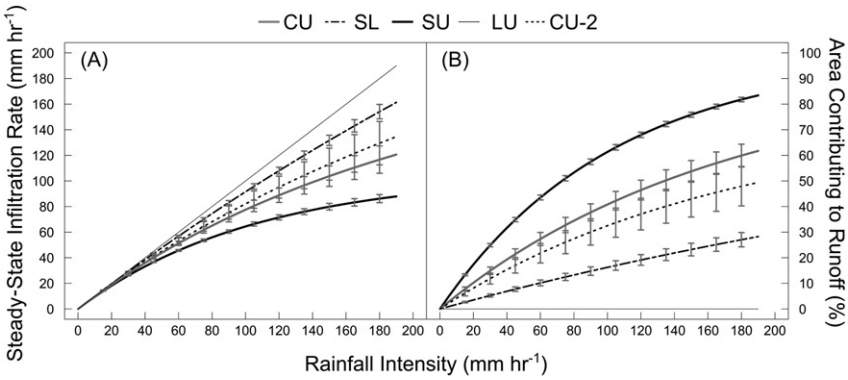

Figure 3. A, Steady-state infiltration rate plotted as a function of rainfall intensity for the five sites. The response of the LU site is equal to the 1:1 line. **B,** Percentage of the plot area contributing to runoff for a given rainfall intensity. Error bars represent the standard error.

contributing to runoff at the highest applied rainfall intensity. This is compared with less than a third (28%) of the plot area contributing to runoff for the same rainfall intensity at the SL site. CU and CU-2 fall in the middle of these two sites with 62% and 49% of the area contributing to runoff, respectively. LU had 0% area contributing to runoff at the highest rainfall intensity.

With the CU-2 site exhibiting a high degree of variability in hydrologic response across the hillslope plots, two separate ANOVA tests were conducted with and without the CU-2 dataset (Fig. 4). Q_{peak} was statistically different across all four sites when CU-2 was excluded. These site differences were still preserved with the addition of CU-2; however, no statistical difference was found between CU and CU-2. Averages for C show a dichotomy in the sites, where CU and SU on average have a higher fraction of applied rainfall turning into runoff compared with SL and LU. This pattern also remains with the addition of the CU-2 site, but CU and SL become indistinguishable from CU-2. Excluding the CU-2 dataset, the trend for the differences between sites is preserved for all five of the steady-state infiltration rates, with a few exceptions. SS2 and SS3 have identical results in which SL and LU are grouped together and different from the remaining two sites. When the steady-state infiltration rates are higher (SS4 and SS5), the uniqueness of the LU site emerges and all sites become statistically different. It is important to note that for SS1, some of the observed differences are a result of the applied rainfall rate. For example, the analysis shows that the steady-state infiltration rate for SL is statistically higher than that of CU (both with and without the CU-2 dataset). This is due to the fact that the lowest applied rainfall intensity for 2014 was 49 mm hr^{-1} and 53 mm hr^{-1} for 2015. Both sites are infiltrating water at a rate that equally matches the application rate (i.e., no runoff). It is likely that if an equal intensity was applied to the plots, there would be no differences between the two sites. In general, addition of the steady-state infiltration rates from CU-2 site results in two main changes: 1) there is no significant difference between CU and CU-2 and 2) there is no significant difference between SL and LU.

Vegetation characteristics (Table 4) were used as explanatory variables for the regression equations (Table 5). These equations explain a large amount of the variation in hydrologic response across sites. Ground cover characteristics were the only variables to emerge as being significant in the modeling process. Among these variables, moss and bare soil were consistently identified as important cover parameters for describing both runoff and infiltration processes. On average, these simple two- and three-parameter regression equations explain 82% of the variability in steady-state infiltration rates, excluding SS1. A poor fit for SS1 is attributed to the fact that out of the 20 plots tested, 14 infiltrated at a rate equal to the applied rainfall rate. This leads to an insufficient amount of variability among sites to fit through the regression procedure. The fits improve for Q_{peak} and C with explained variability of 84% and 85%, respectively.

Discussion

Our rainfall simulation results demonstrate the variability in hydrologic response as a function of ES characteristics. Site response ranged from consistently producing runoff at each applied rainfall rate (SU) to infiltrating the entire applied rainfall volume, resulting in no runoff (LU). Response curves for steady-state infiltration and area contributing to runoff (see Fig. 3), as well as ANOVA results (see Fig. 4), indicate the following sequence of increasing site infiltration capacity: SU, CU, CU-2, SL, and LU. This is consistent with work by Perlinski et al. (2016), which monitored natural runoff response from the same ecological sites (excluding CU-2). High R^2 values of 0.78 — 0.85 for the regression equations (Table 5) illustrate the effectiveness of using pooled data across all five ESs to explain this variability. As previously mentioned, little confidence can be placed in the regression results for SS1 and the results are therefore excluded from this discussion. Site-specific regression equations have been shown to improve the ability to predict hydrological processes compared with lumped equations (Spaeth et al. 1996; Pierson et al.

Table 3
Maximum spatially averaged infiltration rate (μ_f) values for the five study sites. Normal averages and coefficients of variations (CV) are computed using all 4 plots. Adjusted averages and CVs are computed after removing anomalous plots.

	μ_f (mm hr^{-1})				Normal		Adjusted	
Ecological Site	Plot 1	Plot 2	Plot 3	Plot 4	Average (SE)	CV (%)	Average (SE)	CV (%)
CU	130	430	178	163	225 (69.0)	61.2	157.0 (14.2)[1]	15.6[1]
SL	471	361	645	1312	697 (213.1)	61.1	492.3 (82.7)[2]	29.1[2]
SU	89	112	116	106	106 (5.9)	11.3	—[3]	—
LU	Inf[5]	Inf	Inf	Inf	—	—	—	—
CU-2	124	221	4184	224	1188 (998.9)	168.12	189.7 (32.8)[4]	30.0[3]

[1] Values excluding CU plot 2.
[2] Values excluding SL plot 4.
[3] Value not calculated.
[4] Values excluding CU-2 plot 3
[5] μ_f is effectively infinite (i.e., steady-state infiltration rate is equal to the applied rainfall rate).

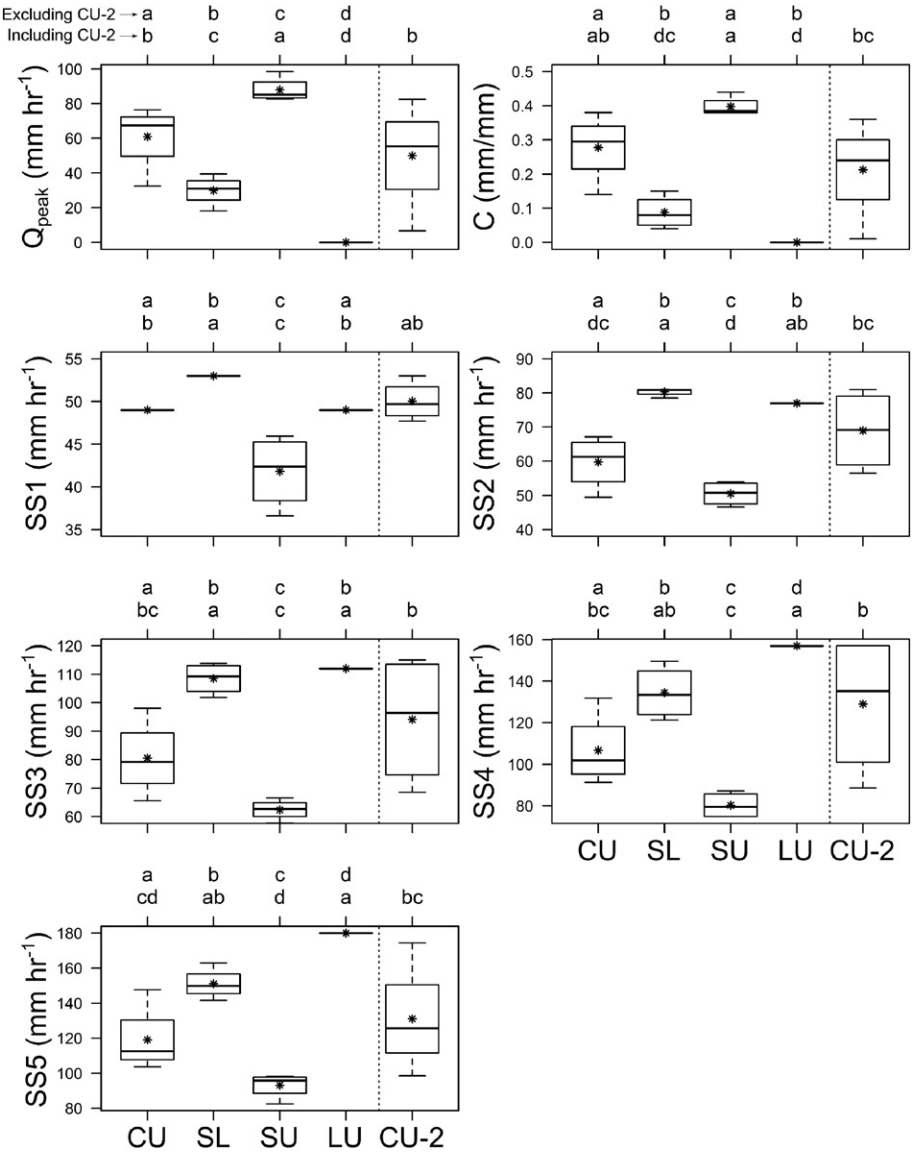

Figure 4. Box and whisker plots for the hydrological variables of interest: peak runoff rate (Q_{peak}), runoff ratio (C), and the five steady-state infiltration rates (SS1-SS5). Average values are indicated by an asterisk. Sites with different lowercase letters are statistically different ($P \leq 0.05$). The two lines of letters distinguish the different ANOVA tests (i.e., including [bottom] and excluding [top] the CU-2 site).

2002). For our experiments an insufficient number of data points prevented the development of site-specific equations. However, our results suggest that simple, more universal equations containing only ground cover characteristics can be used to describe hydrologic process at multiple locations within the UCCW. This can be attributed to the fact that the structure of the plant community is fairly consistent across our study locations, with the exception of the LU site (see Table 4). Various graminoid species are typically intermixed with two dominant species of small subshrubs: fringed sagewort (*Artemisia frigida* Willd) and threetip sagebrush (*Artemisia tripartita* Rydb). There is no statistical difference in grass cover across sites, and only the CU-2 site had a significantly lower amount of shrub cover (see Table 4). Therefore, ground cover characteristics emerged as being the only important variables for explaining these differences.

Two ground cover variables were consistently identified as significant: 1) lesser spikemoss and (2) bare soil. Lesser spikemoss was the most influential variable in each of the equations as indicated by the beta weights (see Table 5). This vascular plant grows as a dense mat with a network of fine roots extending 2–5 cm below the soil surface (Coupland and Johnson 1965). Low water-use requirements make it prevalent in rangeland systems, affecting the structure and composition of plant communities (Colberg and Romo 2003; Romo 2011). It has been noted that this cryptogam can act as a sponge during rainfall events, preventing moisture from reaching surrounding vegetation (Majorowicz 1963). Observations during field experiments suggest that once these plants absorb a small amount of moisture, they effectively create impervious patches in which rainfall is directly converted into surface runoff. The amount of lesser spikemoss present at these sites is negatively correlated with SS infiltration rates and positively with C and Q_{peak} (see Table 5). Bare soil is also negatively correlated with infiltration. This strong negative relationship has been noted by a number of different authors (Branson and Owen 1970; Blackburn 1975; Pierson et al. 2002). Minimal organic matter, lack of root systems, high overland flow velocities, and the sealing of the soil surface due to particles dislodged from rainfall impact are all factors that contribute to the reduced infiltration rates of these areas. For SS4, SS5, Q_{peak}, and C, bare soil was the second most influential variable.

A combination of lesser spikemoss and bare soil cover is the basis for all of the regression relationships. For SS4 and SS5, these two variables alone make up the equations and can explain 78% and 82% of the

Table 4
Ground and canopy cover characteristics for the 20 runoff plots.

		Ground cover (%)						Canopy cover (%)				
Site	Plot	Bare soil	Rock[1]	Litter	Moss[2]	Plant base	Exposed rock[3]	Grass	Shrub[4]	Forb	Sedge	No canopy
CU	1	11.6	10.8	32.4	38.2	7.1	0.0	17.9	18.9	5.5	0.0	57.6
CU	2	11.6	20.5	45.0	12.1	10.8	0.0	45.3	17.6	1.8	4.5	30.8
CU	3	10.8	12.4	32.1	30.1	13.7	0.0	50.3	17.1	6.6	2.9	23.2
CU	4	4.2	8.7	26.6	46.6	14.0	0.0	30.0	11.3	12.6	0.0	46.1
SL	1	4.7	9.2	30.5	34.7	20.8	0.0	33.7	20.8	15.3	0.0	30.3
SL	2	6.8	10.3	55.3	6.3	21.3	0.0	43.4	26.1	6.8	0.0	23.7
SL	3	8.2	12.9	47.6	13.4	17.9	0.0	35.8	27.4	11.6	0.0	25.3
SL	4	4.2	19.5	41.6	22.9	11.8	0.0	43.7	15.5	13.9	0.0	26.8
SU	1	7.9	0.0	53.7	21.6	16.8	0.0	43.7	11.8	20.8	0.0	23.7
SU	2	10.3	6.8	33.2	38.4	11.3	0.0	57.9	9.2	9.5	0.0	23.4
SU	3	13.7	3.4	30.5	43.7	8.7	0.0	46.1	18.4	6.6	0.0	28.9
SU	4	7.1	6.6	44.2	35.5	5.8	0.8	37.1	16.3	6.1	0.0	40.5
LU	1	17.6	0.5	64.0	0.0	16.1	1.8	18.4	38.9	17.9	8.9	15.8
LU	2	7.4	0.5	81.6	0.0	9.0	1.6	17.9	50.5	5.0	14.7	11.8
LU	3	6.6	1.6	87.6	0.0	4.2	0.0	51.8	29.5	10.3	4.7	3.7
LU	4	4.5	0.0	92.1	0.0	3.4	0.0	54.2	31.1	5.0	1.1	8.7
CU-2	1	4.2	4.0	31.8	52.1	7.9	0.0	40.5	5.8	5.5	0.0	48.2
CU-2	2	2.1	8.2	32.4	47.4	10.0	0.0	34.5	11.6	9.2	0.0	44.7
CU-2	3	3.2	7.6	68.2	7.6	13.4	0.0	89.7	4.5	1.3	0.0	4.5
CU-2	4	7.1	5.0	41.6	26.6	19.7	0.0	88.9	0.5	5.3	0.0	5.3

[1] Rock cover is considered to be rock fragments > 2 cm in diameter.
[2] Lesser spikemoss (*Selaginella densa* Rydb).
[3] Granitic boulders exposed at the soil surface.
[4] Small subshrubs (*Artemisia frigida* Willd and *Artemisia tripartita* Rydb) for CU, SL, SU, and CU-2. Big sagebrush (*Artemisia tridentata* Nutt) for LU.

variability, respectively. At these steady-state infiltration rates the applied rainfall rate is quite large and a parsimonious model that ultimately characterizes the fraction of the plot with low infiltration areas (i.e., percent cover of lesser spikemoss and bare soil) is sufficient for explaining a large degree of the variability in infiltration. For the lower intensities the regression relationships for SS2, SS3, and Q_{peak} (see Fig. 4) require slightly more complex three-parameter models and variables like litter, plant base, and rock become significant. In our experiments plant base and rock cover were positively correlated with infiltration. Plant base is a proxy for standing biomass, and therefore root systems that aid in the infiltration of water and the increased roughness of the soil surface due to rock fragments favor greater and more rapid infiltration (Cerdà 2001). Although others have shown that litter cover increases infiltration (Meeuwig 1970; Wilcox et al. 1988), our results suggest a negative relationship.

In addition to describing the difference in hydrologic response across ES, these relationships prove useful for explaining within-site variability. Fitted μ_f values (see Table 3) show that the maximum spatially averaged infiltration rate at some sites can vary substantially from plot to plot. While adjusting the average μ_f value by removing anomalous plots provides a more representative estimate of site-specific infiltration capacity, these anomalous plots are well predicted by the regression equations. For example, CU plot 2 and CU-2 plot 3 have μ_f values 1.7 and 21 times greater than the average μ_f value for the remaining three plots at the sites, respectively. These plots therefore have higher steady-state infiltration rates and lower Q_{peak} and C values. In each case, the lack of lesser spikemoss coverage can explain this increase in infiltration. The CU site on average has 38.6% moss coverage while CU-2 has 42.0%. In contrast, CU plot 2 had 12% moss coverage and CU-2 plot 3 had 7.6% (see Table 4).

As aforementioned, the CU-2 site is unique in this study in that it is not a distinct ES but rather a different state of the CU STM. CU can be considered a mixed-shrub/grass plant community with approximately 36% of the vegetation being grasses and 16% being shrubs. Sandberg bluegrass is the dominant vegetation species. While the ESD indicates a big sagebrush component, vegetation transects showed that fringed sagewort and threetip sagebrush are the dominate shrub species (see Table 4). The CU-2 site represents a more historic climax plant community that evolved with grazing (NRCS 2014). Grasses on average make up approximately 63% of the vegetation with bluebunch wheatgrass being the most prominent species. Shrubs are not as significant to the plant community as in the CU state. CU and CU-2 are the same ESs; however, shifts in the state can alter the plant community and in return influence the hydrologic response of this landscape unit. Including CU-2 in the ANOVA analysis (see Fig. 4) results in no statistical difference between CU and CU-2 for any of the hydrological parameters, yet the variability in response increases. It may also be possible that CU-2 is transitioning either toward or away from the CU site. For example,

Table 5
Forward regression equations for the wet simulator runs using vegetation transect data as the explanatory variables and the five steady-state infiltration rates (SS1-SS5), runoff coefficient (C), and peak runoff rate (Q_{peak}) as the dependent variables. All equations are significant at the $P \le 0.05$ level. Explanatory variables are shown with beta weights.

Variable	SS1 (mm hr^{-1})	SS2 (mm hr^{-1})	SS3 (mm hr^{-1})	SS4 (mm hr^{-1})	SS5 (mm hr^{-1})	Q_{peak} (mm hr^{-1})	C (mm mm^{-1})
Intercept	50.25[1]	78.73[1]	171.52[1]	168.01[1]	191.39[1]	−10.52	−0.57[2]
Variable 1	0.34 Plant Base[3]	−0.52 Moss[1]	−1.53 Moss[1]	−1.40 Moss[3]	−1.61 Moss[1]	1.10 Moss[3] (0.63)	0.01 Moss[1]
(beta weight)	(0.54)	(−0.79)	(−1.39)	(−0.89)	(−0.91)		(1.28)
Variable 2	−0.41 Bare Soil[3]	0.87 Plant Base[3]	−2.17 Bare Soil[1]	−1.71 Bare Soil[4]	−1.98 Bare Soil[2]	3.48 Bare Soil[3]	0.02 Bare Soil[1]
(beta weight)	(−0.49)	(0.39)	(−0.43)	(−0.24)	(−0.25)	(0.47)	(0.60)
Variable 3	−0.07 Moss[2]	−1.12 Bare Soil[3]	−0.54 Litter[2]			−1.52 Rock[4]	0.01 Litter[2]
(beta weight)	(−0.39)	(−0.37)	(−0.55)			(−0.29)	(0.58)
R^2	0.62	0.84	0.85	0.78	0.82	0.84	0.85

[1] $P \le 0.0001$.
[2] $P \le 0.01$.
[3] $P \le 0.001$.
[4] $P \le 0.05$.

vegetation characteristics and consequently the hydrologic response for plots 1 and 2 closely resemble that of the CU site. Quantifying this range in response is important for effectively using the ES concept to model hydrologic processes.

Site-specific hydrologic interactions must also be addressed as a source of variability not explained by the regression equations. The LU site, for instance, is unique compared with the other four sites in its parent material, structure of the plant community, and soil properties (see Table 1). The site has 90% canopy cover, 42% of which is big sagebrush (*Artemisia tridentata* Nutt), creating a sagebrush shrub-interspace complex consisting of different surface microsites (Pierson et al. 1994). There is no evidence of lesser spikemoss at the site due to the fact that the soils were derived from metasedimentary rock instead of granite (Beetle 1956). Differences in runoff and infiltration were observed for these different microsites. During simulation runs, water ponded on the soil surface of the interspaces quicker than any of the other four sites. As water migrated from these interspaces to the shrub areas, infiltration occurred rapidly. Additional rainfall simulation runs (not presented in this paper) were conducted at this site in the fall of 2015, in which the applied rainfall intensity was as high as 311 mm hr^{-1}. Again, no runoff was observed on any of the four plots tested. This suggests that this site effectively never exhibits Hortonian overland flow under natural conditions and is instead dominated by subsurface processes driven by the high infiltration capacity of the big sagebrush areas (Ryel et al. 2003; Eldridge and Rosentreter 2004).

The shallow ESs (SU and SL) also exhibit distinct site characteristics that are important for understanding the hydrologic response. Geophysical measurements suggest that SU has the smallest average depth to fractured bedrock of all the sites (see Table 1). Moreover, large granite boulders are intermixed within the soil profile and are often exposed at the soil surface. Localized regions of saturation due to these impervious zones in the subsurface were evident during simulation runs. SU plot 1, for example, has a large granite boulder approximately 1.2 m below the soil surface that spans the length of the runoff plot. Reflectometer probes showed that before simulator runs, the region above this granite layer was at 34% water content. During the wet runs, water content increased by only 1.4%. Furthermore, this plot yielded significant steady-state runoff (16.4 mm hr^{-1}) during the dry run. Therefore, saturation excess due to impervious regions of the subsurface may help explain why SU plot 1 had the highest C (0.44) and Q_{peak} (98.5 mm hr^{-1}) of the 20 plots tested. At the SL site the infiltration capacity is large (see Fig. 3), second only to LU. Plot 4, however, has a C of just 0.04 compared with an average C of 0.11 for the remaining three plots. The density of pocket gopher burrows on this plot may help to explain this trend. The average density of these burrows was 0.25 m^{-2} for plots 1–3 while 1.7 m^{-2} for plot 4. Tagging the surface runoff using dye tabs showed water preferentially infiltrating into these burrows.

Conclusion

In this study, a dataset of extensive field observations was developed using variable-intensity rainfall simulation runs that directly relate hydrologic response to rangeland ES characteristics. We showed that characteristics of ESs in a given state could be used to quantify the variability in hydrologic response across a semiarid rangeland watershed in southeastern Wyoming. While some sites exhibited spatially variable μ_f values at the plot scale, we computed meaningful site average values that outlined the differences in the maximum infiltration capacity at the ES scale. Moreover, we derived parsimonious equations consisting only of ground cover variables (e.g., moss cover, bare soil, and litter) capable of explaining, on average, 83% of the variability in response across sites. Additional site-specific characteristics explain the remaining variability. A large runoff response was measured at the SU site due to a high percentage of moss cover and localized saturation areas from impervious granite corestones buried at the near surface. In contrast, the dense, big sagebrush of the LU site easily infiltrated any ponded water that formed during simulation runs, resulting in no measurable runoff at this site. Runoff-infiltration processes were not statistically different for two different states of an ES (i.e., CU and CU-2), but the degree of variability in response increased for CU-2 comparatively. Quantifying this range in ES hydrologic response is critical to understand rangeland watersheds and their potential for being impacted by climate and management practices.

Management Implications

The ES concept is a well-established framework for partitioning rangelands into homogeneous land units on the basis of soil, vegetation, and climatic similarities for the purpose of monitoring and assessment (Brown 2010). Detailed quantitative datasets are necessary to predict functional feedbacks among ecological site characteristics, hydrologic processes, and the resilience of states and community phases and functional thresholds (Briske et al. 2008; Peterson et al. 1998; Perlinski et al. 2016; Williams et al. 2016). Rainfall simulation provides a controlled environment in which these datasets can be acquired. Integrating these datasets into evolving tools like ESDs, STMs, and rangeland assessment models, such as RHEM, will improve our ability to understand and manage the complex ecohydrologic processes on rangelands.

It is important to acknowledge that improved ES mapping and detailed development of ESDs is needed, particularly in southeastern Wyoming, in order to assess these functional feedbacks on a large scale. While we have used UCCW as a test site for this study, we propose that this method can be used to characterize the hydrologic response for a range of ESs within a broader MLRA, provided that detailed mapping is available. We also stress the need for replication at the ES scale. Although our plots represent subsamples of a given ES, measuring the hydrologic response of the same ES at different locations within a given MLRA would improve our ability to ascertain the characteristic hydrologic response of a given ES. With more robust tools, the management of water resources for a variety of rangeland settings while accommodating for the dynamics and uncertainty associated with stressors such as climate change and population growth can be improved.

Acknowledgments

We thank David Legg for helpful conversations and Andrew Annear for help with field work.

Literature Cited

Archer, SR, Predick, KI, 2008. Climate change and ecosystems of the southwestern United States. Rangelands 30, 23–28.
Beetle, AA, 1956. Range survey in Wyoming's Big Horn Mountains. Wyoming Agriculture Experiment Station, Laramie, WY, USA Bulletin 341. 40 p.
Blackburn, WH, 1975. Factors influencing infiltration and sediment production of semiarid rangelands in Nevada. Water Resour. Res. 11, 929–937.
Briske, DD, Fuhlendork, SD, Smeins, FE, 2008. State-and-transition models, thresholds, and rangeland health: A synthesis of ecological concepts and perspectives. Rangel. Ecol. Manag 58, 1–10.
Branson, FA, Owen, JB, 1970. Plant cover, runoff, and sediment yield relationships on Mancos Shale in western Colorado. Water Resour. Res. 6, 783–790.
Brown, J, 2010. Ecological sites: their history, status and future. Rangelands 32, 5–8.
Burns, IS, Guertin, DP, Goodrich, DC, 2010. Multi-scale calibration of KINEROS-DWEPP, a combined physically-based hydrologic model and process-based soil erosion model. Second Joint Federal Interagency Conference, Las Vegas, NV, USA.
Campbell Scientific Inc, 2011. Instruction manual: wireless sensor network. Available at: https://s.campbellsci.com/documents/us/manuals/wireless-sensor-network.pdf Accessed 1 May 2014.
Cerdà, A, 2001. Effects of rock fragment cover on soil infiltration, interrill runoff and erosion. Eur. J. Soil Sci. 52, 59–68.
Chauvin, GM, Flerchinger, GN, Link, TE, Marks, D, Winstral, AH, Seyfried, MS, 2011. Long-term water balance and conceptual model of a semi-arid mountainous catchment. J. Hydrol. 400, 133–143.
Colberg, TJ, Romo, JT, 2003. Clubmoss effects on plant water status and standing crop. J. Range Manag. 56, 489–495.
Coupland, RT, Johnson, RE, 1965. Rooting characteristics of native grassland species in Saskatchewan. J. Ecol. 53, 475–507.

Eldridge, DJ, Rosentreter, R, 2004. Shrub mounds enhance water flow in a shrub-steppe community in southwestern Idaho, U.S.A. Proceedings RMRS-P-31. Ogden, UT, USA: USDA Forest Service, pp. 77–83.
Flerchinger, GN, Cooley, KR, 2000. A ten-year water balance of a mountainous semi-arid Watershed. J. Hydrol. 237, 86–99.
Frost, CD, Frost, BR, Chamberlain, KR, Edwards, BR, 1999. Petrogenesis of the 1.43 Ga Sherman batholith, SE Wyoming, USA: a reduced, rapakivi-type anorogenic granite. J. Petrology 40, 1771–1802.
Gee, GW, Or, D, 2002. Porosity. In: Dane, J., Topp, C. (Eds.), Methods of soil analysis: Part 4-physical methods. Soil Science Society of America, Madison, WI, USA, pp. 241–254.
Hartley, HO, 1950. The use of range in analysis of variance. Biometrika 37, 271–280.
Havstad, K, Peters, D, Allen-Diaz, B, Bartolome, J, Bestelmeyer, B, Briske, D, Brown, J, Brunson, M, Herrick, J, Huntsinger, L, Johnson, P, Joyce, L, 2009. The western United States rangelands: a major resource. In: Wedin, W.F., Fales, S.L. (Eds.), Grassland: quietness and strength for a new American agriculture. Soil Science Society of America, Madison, WI, USA, pp. 75–93.
Hawkins, RH, 1982. Interpretations of source area variability in rainfall-runoff relations. In: Singh, V.P. (Ed.), Rainfall-runoff relationships. Water Resources Publications, Littleton, CO, USA, pp. 303–324.
Hayes, MM, Miller, SN, Murphy, MA, 2014. High-resolution landcover classification using Random Forest. Remote Sens. Lett. 5, 112–121.
Hernandez, M, Nearing, MA, Stone, JJ, Pierson, FB, Wei, H, Spaeth, KE, Heilman, P, Weltz, MA, Goodrich, DC, 2013. Application of a rangeland soil erosion model using National Resources Inventory data in southeastern Arizona. J. Soil Water Conserv. 68, 512–525.
Herrick, JE, Van Zee, JW, Havstad, KM, Burkett, LM, Whitford, WG, 2005. Monitoring manual for grassland, shrubland and savanna ecosystems Vol II: Design, supplementary methods and interpretation. USDA-ARS Jornada Experimental Range, Las Cruces, New Mexico. The University of Arizona Press, Tucson, AZ.
Kleinbaum, DG, Kupper, LL, Muller, KE, 1988. Applied regression analysis and other multivariable methods. second ed. PWS-KENT, Boston, MA, USA.
Loague, K, Gander, GA, 1990. Spatial variability of infiltration on a small rangeland catchment. Water Resour. Res. 26, 957–971.
Majorowicz, AK, 1963. Clubmoss infestation on northeastern Montana rangeland. Proc. Annu. Meet. Am. Soc. Range Manag. 16, 72.
Meeuwig, RO, 1970. Infiltration and soil erosion as influenced by vegetation and soil in northern Utah. J. Range Manag. 23, 185–188.
Nearing, MA, Wei, H, Stone, JJ, Pierson, FB, Spaeth, KE, Weltz, MA, Flanagan, DC, Hernandez, M, 2011. A rangeland hydrology and erosion model. Trans. Am. Soc. Agric. Biol. Eng. 54, 901–908.
Newman, BD, Wilcox, BP, Archer, SR, Breshears, DD, Dahm, CN, Duffy, CJ, McDowell, NG, Phillips, FM, Scanlon, BR, Vivoni, ER, 2006. Ecohydrology of water-limited environments: a scientific vision. Water Resour. Res. 42, 1–15.
NRCS (Natural Resources Conservation Service), 2013. Ecological Site Description (ESD) System for rangeland and forestland. Available at: https://esis.sc.egov.usda.gov/Welcome/pgESDWelcome.aspx.
NRCS (Natural Resources Conservation Service), 2014. Ecological Site Description System. Available at: https://esis.sc.egov.usda.gov/Welcome/pgReportLocation.aspx?type=ESD Accessed 15 March 2015.
Osborn, HB, Lane, L, 1969. Precipitation-runoff relations for very small semiarid rangeland watersheds. Water Resour. Res. 5, 419–425.
Paige, GB, Stone, JJ, 1996. Measurement methods to identify and quantify the spatial variability of infiltration on rangelands. Proceedings of ARS Workshop, Real World Infiltration, July 22–25. Colorado Water Resources Research Institute, Pingree Park, CO, USA, pp. 109–122 Information Series 86.
Paige, GB, Stone, JJ, Smith, JR, Kennedy, JR, 2003. The walnut gulch rainfall simulator: a computer-controlled variable intensity rainfall simulator. Appl. Eng. Agric. 20, 25–31.
Perlinski, A. T., G. B. Paige, S. N. Miller, and A. L. Hild. 2016. Hydrologic response of four ecological sites to natural rainfall events within a semi-arid watershed. Unpublished results.
Peterson, G, Allen, CR, Holling, CS, 1998. Ecological resilience, biodiversity and scale. Ecosystems 1, 6–18.
Pierson, FB, Spaeth, KE, Weltz, MA, Carlson, DH, 2002. Hydrologic response of diverse western rangelands. J. Range Manag. 55, 558–570.
Pierson, FB, Van Vactor, SS, Blackburn, WH, Wood, JC, 1994. Incorporating small scale spatial variability into predictions of hydrologic response on sagebrush rangelands. In: Blackburn, W.H., Schuman, G.E., Pierson, F.B. (Eds.), Variability in rangeland water erosion processes. Soil Science Society of America, Madison, WI, USA, pp. 23–34.
Pilgrim, DH, Chapman, TG, Doran, DG, 1988. Problems of rainfall-runoff modeling in arid and semiarid regions. Hydrol. Sci. J. 33, 379–400.
Polley, HW, Briske, DD, Morgan, JA, Wolter, K, Bailey, DW, Brown, JR, 2013. Climate change and North American rangelands: trends, projections, and implications. Rangel. Ecol. Manag. 66, 493–511.
Pyke, DA, Herrick, JE, Shaver, P, Pellant, M, 2002. Rangeland health attributes and indicators for qualitative assessment. J. Rangel. Manag. 55, 584–597.
R Development Core Team, 2014. R: a language and environment for statistical computing. R Foundation for Statistical Computing, Vienna, Austria.
Romo, JT, 2011. Clubmoss, precipitation, and microsite effects on emergence of graminoid and forb seedlings in the semiarid Northern Mixed Prairie of North America. J. Arid Environ. 75, 98–105.
Ryel, RJ, Caldwell, MM, Leffler, AJ, Yoder, CK, 2003. Rapid soil moisture recharge to depth by roots in a stand of Artemisia Tridentata. Ecology 84, 757–764.
SAS Institute [computer program], 2013. SAS Software version 9.4. SAS Institute, Cary, NC, USA.
Seyfried, MS, 1991. Infiltration patterns from simulated rainfall on a semiarid rangeland soil. Soil Sci. Soc. Am. J. 55, 1726–1734.
Simanton, JR, Rawitz, E, Shirley, ED, 1984. Effects of rock fragments on erosion of semiarid rangeland soils. In: Kral, D.M., Hawkins, S.L. (Eds.), Erosion and productivity of soils containing rock fragments. Soil Science Society of America, Madison, WI, USA, pp. 65–72.
Simanton, JR, Weltz, MA, Larsen, HD, 1991. Rangeland experiments to parameterize the water erosion prediction project model: vegetation canopy cover effects. J. Range Manag. 44, 276–282.
Sivapalan, M, 2003. Process complexity at hillslope scale, process simplicity at the watershed scale: is there a connection? Hydrol. Process 17, 1037–1041.
Skinner, QD, Speck Jr., JE, Smith, M, Adams, JC, 1984. Stream water quality as influenced by beaver within grazing systems in Wyoming. J. Range Manag. 37, 142–146.
Spaeth, KE, Pierson, FB, Weltz, MA, Awang, JB, 1996. Gradient analysis of infiltration and environmental variables as related to rangeland vegetation. Trans. Am. Soc. Agric. Eng. 39, 67–77.
Stone, JJ, Paige, GB, 2003. Variable rainfall intensity rainfall simulator experiments on semi-arid rangelands. In: Renard, K.G., McElroy, S., Gburek, W., Canfield, E., Scott, R.L. (Eds.), Proceedings of the First Interagency Conference on Research in the Watersheds. USDA Agricultural Research Service, Washington, DC, USA, pp. 83–88.
Stone, JJ, Paige, GB, Hawkins, RH, 2008. Rainfall intensity-dependent infiltration rates on rangeland rainfall simulator plots. Trans. Am. Soc. Agric. Eng. 51, 45–53.
Taucer, PI, Munster, CL, Wilcox, BP, Owens, MK, Mohanty, BP, 2008. Large-scale rainfall simulation experiments on juniper rangelands. Trans. Am. Soc. Agric. Biol. Eng. 51, 1951–1961.
Tukey, JW, 1953. Some selected quick and easy methods of statistical analysis. Trans. N. Y. Acad. Sci. 16, 88–97.
Turnbull, L, Wainwright, J, Brazier, RE, 2008. A conceptual framework for understanding semi-arid land degradation: ecohydrological interactions across multiple-space and time scales. Ecohydrology 1, 23–34.
USDA (US Department of Agriculture), 2013. Interagency ecological site description handbook for rangelands. United States Department of Agriculture, Washington, DC, USA 109 p.
USDA (US Department of Agriculture), Forest Service, 2013. Pole Mountain vegetation project notice of proposed action. Medicine Bow-Routt National Forests, Laramie WY, USA Available at: http://www.fs.fed.us/nepa/nepa_project_exp.php?project=41662. Accessed 16 January 2014.
Wilcox, BP, Breshears, DD, Allen, CD, 2003. Ecohydrology of a resource- conserving semiarid woodland: effects of scaling and disturbance. Ecol. Monogr. 73, 223–239.
Wilcox, BP, Rawls, WJ, Brakensiek, DL, Wight, JR, 1990. Predicting runoff from rangeland catchments: a comparison of two models. Water Resour. 26, 2401–2410.
Wilcox, BP, Wood, MK, Tromble, JM, 1988. Factors influencing infiltrability of semiarid mountain slopes. J. Range Manag. 41, 197–206.
Williams, CJ, Pierson, FB, Spaeth, KE, Brown, JR, Al-Hamdan, OZ, Weltz, MA, Nearing, MA, Herrick, JE, Boll, J, Robichaud, PR, Goodrich, DC, Heilman, P, Guertin, DP, Hernandez, M, Wei, H, Hardegree, SP, Strand, EK, Bates, JD, Metz, LJ, Nichols, MH, 2016. Incorporating hydrologic data and ecohydrologic relationships into ecological site descriptions. Rangel. Ecol. Manag. 69, 4–19.
Yu, B, Rose, CW, Coughlan, KJ, Fentie, B, 1997. Plot-scale-runoff characteristics and modeling at six sites in Australia and Southeast Asia. Trans. Am. Soc. Agric. Eng. 40, 1295–1303.